iScience

CellPress
OPEN ACCESS

Article

T cell factor 1 (TCF-1) defines T cell differentiation in colorectal cancer

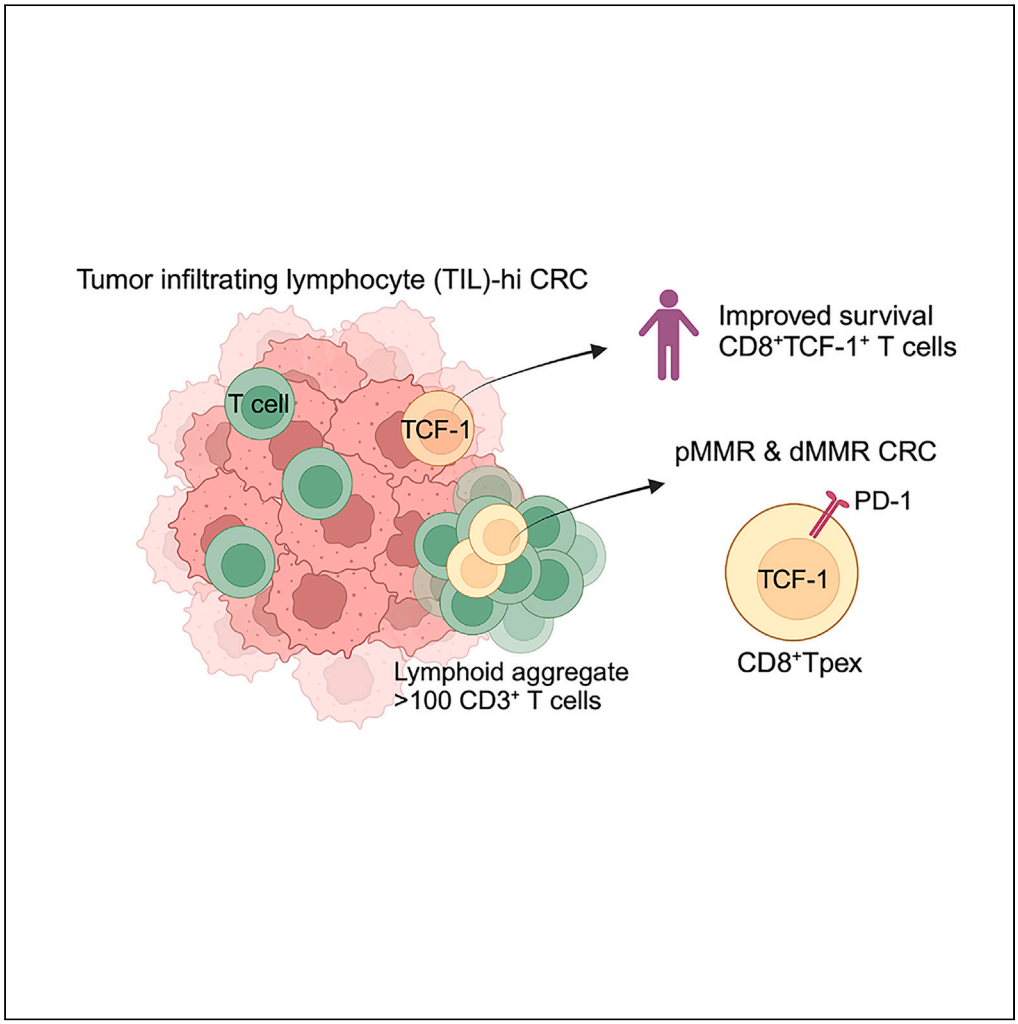

Kelly Tran, Anita N. Kumari, Dinesh Raghu, ..., John Mariadason, David S. Williams, Lisa A. Mielke

lisa.mielke@onjcri.org.au

Highlights

15% of stage III pMMR CRCs have a high frequency of TILs

$CD3^+CD8^+TCF\text{-}1^+$ T cells predict improved survival of stage III CRC patients

Lymphoid aggregates harbor $CD3^+CD8^+TCF\text{-}1^+PD\text{-}1^+$ T_{pex} cells in primary CRCs

T_{pex} cells are abundant in lymphoid aggregates of TIL-hi pMMR and dMMR CRCs

Tran et al., iScience 27, 110754
September 20, 2024
https://doi.org/10.1016/j.isci.2024.110754

iScience

CellPress
OPEN ACCESS

Article

T cell factor 1 (TCF-1) defines T cell differentiation in colorectal cancer

Kelly Tran,[1,2,7] Anita N. Kumari,[1,2] Dinesh Raghu,[1,2] Daniel R.A. Cox,[3,4] Su Kah Goh,[3,4] Marcos V. Perini,[3,4] Vijayaragavan Muralidharan,[3,4] Niall C. Tebbutt,[1,2,3,5] Andreas Behren,[1,2] John Mariadason,[1,2] David S. Williams,[1,2,6] and Lisa A. Mielke[1,2,7,8,*]

SUMMARY

The presence of precursor to exhausted (T_{pex}) $CD8^+$ T cells is important to maintain robust immunity following treatment with immune checkpoint inhibition (ICI). Impressive responses to ICI are emerging in patients with stage II-III mismatch repair (MMR)-deficient (dMMR) colorectal cancer (CRC). We found 64% of dMMR and 15% of mismatch repair-proficient (pMMR) stage III CRCs had a high frequency of tumor infiltrating lymphocytes (TIL-hi). Furthermore, expression of TCF-1 *(Tcf7)* by $CD8^+$ T cells predicted improved patient prognosis and T_{pex} cells ($CD3^+CD8^+TCF\text{-}1^+PD\text{-}1^+$) were abundant within lymphoid aggregates of stage III CRCs. In contrast, $CD3^+CD8^+TCF\text{-}1^-PD\text{-}1^+$ cells were more abundant at the invasive front and tumor core, while γδ T cells were equally abundant in all tumor areas. Interestingly, no differences in the frequency of T_{pex} cells were observed between TIL-hi dMMR and TIL-hi pMMR CRCs. Therefore, T_{pex} cell function and ICI response rates in TIL-hi CRC warrants further investigation.

INTRODUCTION

Colorectal cancer (CRC) is a leading cause of cancer death worldwide and T cells play a key role in preventing the development and progression of these tumors.[1,2] CRCs that have defective DNA mismatch repair (dMMR) capacity (also referred to as microsatellite instability high (MSI-H)) generally produce more neoantigens and elicit a better immune response.[3] In recent years, immune checkpoint inhibition (ICI) with anti-PD-1 and anti-CTLA4 antibodies has been widely used for the successful treatment of dMMR/MSI-H tumors in stage IV metastatic CRC (mCRC).[4,5] Furthermore, ICI is now gaining traction as an effective treatment in earlier stage dMMR CRC, with the first clinical trials revealing impressive response rates in the neoadjuvant setting.[3,6–15]

A critical role of immune cells in the defense against CRC progression is further highlighted by recent studies showing that tumors with high numbers of lymphoid aggregates[16–18] or increased tumor infiltrating lymphocytes (TILs) are associated with better survival outcomes irrespective of MMR status.[19–22] In addition, TILs are predictive of ICI response in mCRC.[23] Interestingly, one of the first clinical trials using neoadjuvant ICI in non-mCRC treating 40 stage I-III CRC patients with ICI, reported pathological responses in 100% of dMMR tumors and 27% of proficient DNA mismatch repair (pMMR) tumors.[6] These response rates are higher than the response rates observed in mCRC.[5,24] Notably, the presence of $CD8^+PD\text{-}1^+$ T cell infiltration was predictive of ICI response, in both the dMMR and pMMR CRC patient groups.[6] In addition to $CD8^+$ T cells, other T cell subsets, including γδ T cells have recently emerged as important players capable of responding to ICI in stage II-III CRC, particularly in dMMR tumors.[25] Together, these studies show that multiple T cell subsets play an important role in defense against CRC and both dMMR and some pMMR CRCs can respond to ICI.[6]

Extending on the findings that γδ T cell and $CD8^+$ T cell infiltration is associated with better patient prognosis,[26–28] recent work from numerous labs has shown that distinct subsets of γδ T cells, including Vδ1 cells in humans and Vγ1 and Vγ7 subsets in mice, play an important role to limit colon tumor growth.[25,28–30] On the other hand, alternate IL-17 producing γδ T cell subsets act to promote tumor growth.[30,31] Intrinsic factors and microenvironment signals regulating γδ T cell anti-tumor properties are now starting to emerge, with microbial, T cell receptor, butyrophilin-like molecules, Natural Killer cell receptors and integrins all recently implicated.[25,29,30,32,33] In addition, recent work by our laboratory and others showed the transcription factor, T cell factor 1 (TCF-1) (encoded by the gene *Tcf7*) acts as a potent suppressor

[1]Olivia Newton-John Cancer Research Institute, Heidelberg, VIC, Australia
[2]School of Cancer Medicine, La Trobe University, Heidelberg, VIC, Australia
[3]Department of Surgery (Austin Precinct), University of Melbourne, Melbourne, VIC, Australia
[4]HPB & Liver Transplant Surgery Unit, Department of Surgery, Austin Health, Heidelberg, VIC, Australia
[5]Department of Medical Oncology, Austin Health, Heidelberg, VIC, Australia
[6]Department of Pathology, Austin Health, Heidelberg, VIC, Australia
[7]La Trobe Institute for Molecular Science, La Trobe University, Bundoora, VIC, Australia
[8]Lead contact
*Correspondence: lisa.mielke@onjcri.org.au
https://doi.org/10.1016/j.isci.2024.110754

of γδ T cell anti-tumor effector functions.[28,34] However, more work is required to determine how these different γδ T cell subsets infiltrate CRCs, their distribution in different tumor subtypes and how inhibitory receptors influence γδ T cell function and response to treatment.

In recent years, detailed investigation of $CD8^+$ T cell differentiation in situations of chronic stimulation, such as cancer or chronic viral infection, have unveiled numerous populations of exhausted $CD8^+$ T cells (T_{ex}) that play a critical role in tumor defense.[2] To mediate early tumor control, naive $CD8^+$ T cells differentiate into short-lived effector T (T_{eff}) cells that express cytotoxic molecules, including granzymes, perforin and cytokines, critical for tumor cell killing.[2] Naive $CD8^+$ T cells also differentiate into precursors of exhausted T (T_{pex}) cells. This cell population is marked by the transcription factor TCF-1, inhibitory receptor PD-1, and as antigen stimulation persists, T_{pex} cells are capable of differentiating into terminally differentiated exhausted $CD8^+$ T cell (T_{tex}) populations.[2,35–37] T_{tex} cells are short-lived terminally differentiated cells and although not as efficient as T_{eff} cells, can produce cytotoxic molecules and significantly contribute to overall tumor control. Investigation of tumor models and chronic viral infections show that T_{pex} cells retain stem-like or progenitor features, expand dramatically in response to ICI and are essential for the overall maintenance of T_{tex} cells.[2,35–38] The identification of T_{pex} cells resolved the long-standing question of how $CD8^+$ T cell populations could be reinvigorated following ICI to eliminate tumor cells. Building on these discoveries in a clinical setting, increased ratios of $TCF\text{-}1^+CD8^+$ cells were shown to be an important predictive factor of response to ICI in melanoma.[39] Continued investigation of T_{pex} cells, also known as stem-like exhausted $CD8^+$ T cells, have confirmed the importance of these cell populations in reinvigorating T cell responses following ICI in numerous cancer types.[39–44] In addition, recent studies have identified T_{pex} cells preferentially localize to lymphoid aggregate or tertiary lymphoid structures in lung cancers,[45–47] however, the presence of T_{pex} cells in the colon and CRC has only recently begun to be explored.[48,49] Reports showing that some T_{pex} cells, particularly those residing in secondary lymphoid organs, express CXCR5.[48,49] The presence of these $CD8^+CXCR5^+$ cells in tumor draining lymph nodes were predictive of better prognosis in stage III CRC.[48,49]

We set out to investigate the overall TIL frequency and T cell differentiation in pMMR vs. dMMR CRCs. We found that 24% of stage III CRC patients had robust TIL infiltration, including 64% of dMMR and 15% of pMMR tumors. Survival analysis demonstrated that TCF-1-expressing $CD8^+$ T cells correlated with better patient survival outcomes in stage III CRC. $CD8^+$ T cell phenotyping in different locations within and surrounding tumors, revealed that a population of $CD8^+TCF\text{-}1^+PD\text{-}1^+$ cells encompassing T_{pex} cells, were significantly more abundant in lymphoid aggregates compared with other areas of the tumor, whereas $CD8^+TCF\text{-}1^-PD\text{-}1^+$ containing populations of activated and T_{ex} cells, were most abundant in the tumor core and invasive front. In contrast, analysis of γδ T cells revealed equal distribution of these cells in each tumor area analyzed. These results highlight differences in $CD8^+$ T cell and γδ T cell spatial distribution in stage III CRC. Our analysis of TIL-hi CRCs revealed no difference in the frequency of $CD8^+TCF\text{-}1^+PD\text{-}1^+$ populations between dMMR and pMMR cohorts. These results suggest that both TIL-hi dMMR and pMMR tumors are capable inducing $CD8^+$ T cell differentiation, including differentiation of $CD8^+TCF\text{-}1^+PD\text{-}1^+$ T_{pex} cells. Overall, our findings warrant further research with larger datasets dissecting the role and mechanisms controlling T_{pex} formation and function in lymphoid aggregates, in addition to γδ T cells in defense against CRC and treatment response.

RESULTS

TILs correlate with MMR status in stage III CRC

The presence of TILs, in particular $CD8^+$ T cells, γδ T cells, and dMMR status are established predictors of improved outcomes for CRC patients.[19,26–28] To begin to establish a relationship between these factors, we determined and classified the TIL status of 411 stage III CRCs as TIL-hi or TIL-lo as previously described[19] and determined TIL association with MMR status. We assessed hematoxylin and eosin (H&E) staining of 411 tumors for the presence of TILs and found that 98 (24%) had a TIL-hi phenotype and 313 (76%) had a TIL-lo phenotype (Figure 1A). Of the 411 tumors analyzed, 74 (18%) had a dMMR phenotype, and 337 (82%) had a pMMR phenotype (Figure 1B; Table S1). Analysis of TILs in conjunction with MMR status, revealed that 64% of dMMR tumors displayed a TIL-hi phenotype. Intriguingly, we observed that 15% of pMMR patients also displayed a TIL-hi phenotype (Figure 1C). Our analysis of MMR status within the overall TIL-hi group, revealed that of the 98 TIL-hi tumors identified, they equally encompassed both dMMR and pMMR tumors (Figure 1D). These results indicate that although the majority of stage III CRCs are TIL-low and pMMR, 24% of tumors exhibited robust TIL infiltration.

$CD8^+$ T cells are abundant in CRC lymphoid aggregates, while γδ T cells are equally distributed in all tumor regions

Given the robust infiltration of TILs observed in a proportion of stage III CRCs, we next set out to perform a more detailed analysis of lymphocyte subsets in these CRCs. $CD8^+$ T cells and γδ T cells play a critical role in defense against CRC and are two of the major cell types involved in immunotherapy response in CRC.[6,25,28] To determine whether the TIL-hi phenotype was also associated with increased T cell infiltration, we assessed total T cells and $CD8^+$ T cells in a small cohort of TIL-hi and TIL-lo stage III CRCs (Figures S1A and S1B). As expected, total T cells and $CD8^+$ T cells were increased in TIL-hi tumors (Figures S1A and S1B). In addition, the number of γδ T cells were also increased in TIL-hi tumors (Figure S1C). We next analyzed both the differentiation status and spatial distribution of γδ T cells and $CD8^+$ T cells in 20 stage III TIL-hi tumors, of which 10 were dMMR and 10 were pMMR. This analysis allowed us to directly compare immune responses in dMMR and pMMR tumors. We assessed the following tumor locations; tumor core, invasive front, lymphoid aggregates (defined by a cluster of >100 $CD3^+$ cells that are in direct contact with one another), tumor stroma and normal-adjacent tissue (Figure 2A). The tumor samples were stained and analyzed using multiplex immunohistochemistry (mIHC) for the following cell markers; CD3, CD8, TCRδ, PanCK and DAPI (Figures 2B–2F).

T cell subset density and percentage frequencies were analyzed for all $CD3^+$ cells (Figure 2G), $CD3^+CD8^+TCR\delta^-$ cells (Figure 2H) and $CD3^+CD8^-TCR\delta^+$ (Figure 2I). We analyzed each cell subset across the five tumor areas of interest, revealing as expected that $CD3^+$ T cells were significantly enriched in lymphoid aggregates (Figure 2G). Lymphoid aggregates were also enriched in TIL-hi vs. TIL-lo tumors

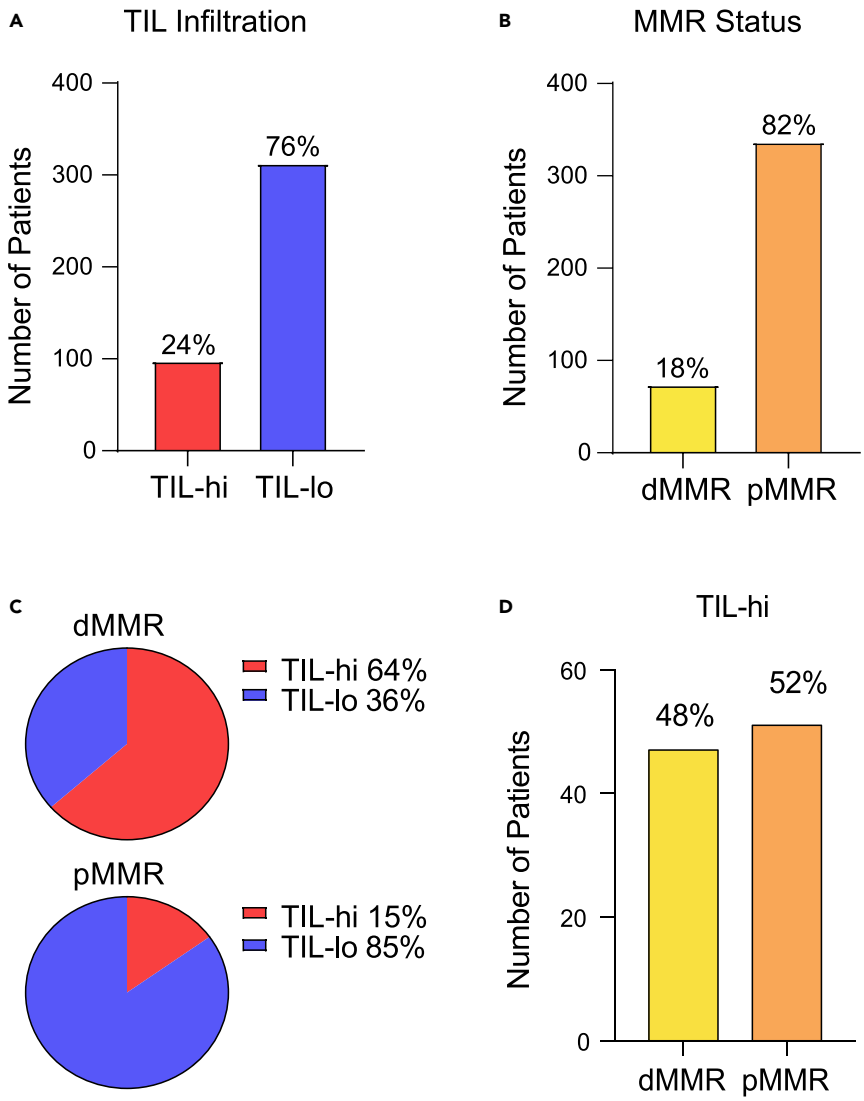

Figure 1. TIL frequency correlates with MMR status in stage III CRC

(A and B) Stage III CRCs were analyzed and stratified as A) TIL-hi or TIL-lo infiltration and for B) MMR status. Data are presented as number of patients and the frequency on each graph represents the percent of patients in each subgroup.

(C) Frequency of TIL-hi and TIL-lo tumors shown for dMMR and pMMR subgroups in stage III CRC.

(D) Number and frequency of dMMR or pMMR patients among TIL-hi stage III CRCs. A total of 411 stage III CRCs were analyzed.

(Figure S1D). Similarly, $CD3^+CD8^+TCR\delta^-$ cells were increased in lymphoid aggregates, compared to the tumor stroma and normal-adjacent tissue (Figure 2H). Comparatively, equivalent frequencies of γδ T cells ($CD3^+CD8^-TCR\delta^+$) were observed across all tumor regions analyzed (Figure 2I). Interestingly, we observed a significant increase in total $CD3^+$ T cells in dMMR lymphoid aggregates and increased frequency of γδ T cells in dMMR tumors, consistent with previous reports[25,50] (Figures 2G–2I; Table S2). These data demonstrate that $CD8^+$ T cells accumulate in dense lymphoid aggregates, whereas γδ T cells are more dispersed throughout the tumor microenvironment.

Different γδ T cell effector subsets localize within the tumor and in the tumor periphery

While our analysis demonstrated that γδ T cells are equally abundant in all tumor regions, we next sought to assess their phenotype in different tumor regions. Recent reports from our laboratory and others identified TCF-1 as a key suppressor of γδ T cell effector function in multiple cancer types, and that low TCF-1 expression efficiently marked effector γδ T cells in tumors.[28,34] The function of inhibitory receptors on γδ T cells, has only recently begun to emerge, with PD-1 expression being associated with enhanced tumor cell killing by human γδ T cells in *in vitro* CRC co-cultures.[25] In addition, studies in mice linked PD-1 expression with IL-17 production and γδ T cell exhaustion.[30,51] Therefore, we analyzed γδ T cells for TCF-1 and PD-1 expression in different tumor regions of our TIL-hi CRC cohort (Figure S2A). Interestingly, mIHC

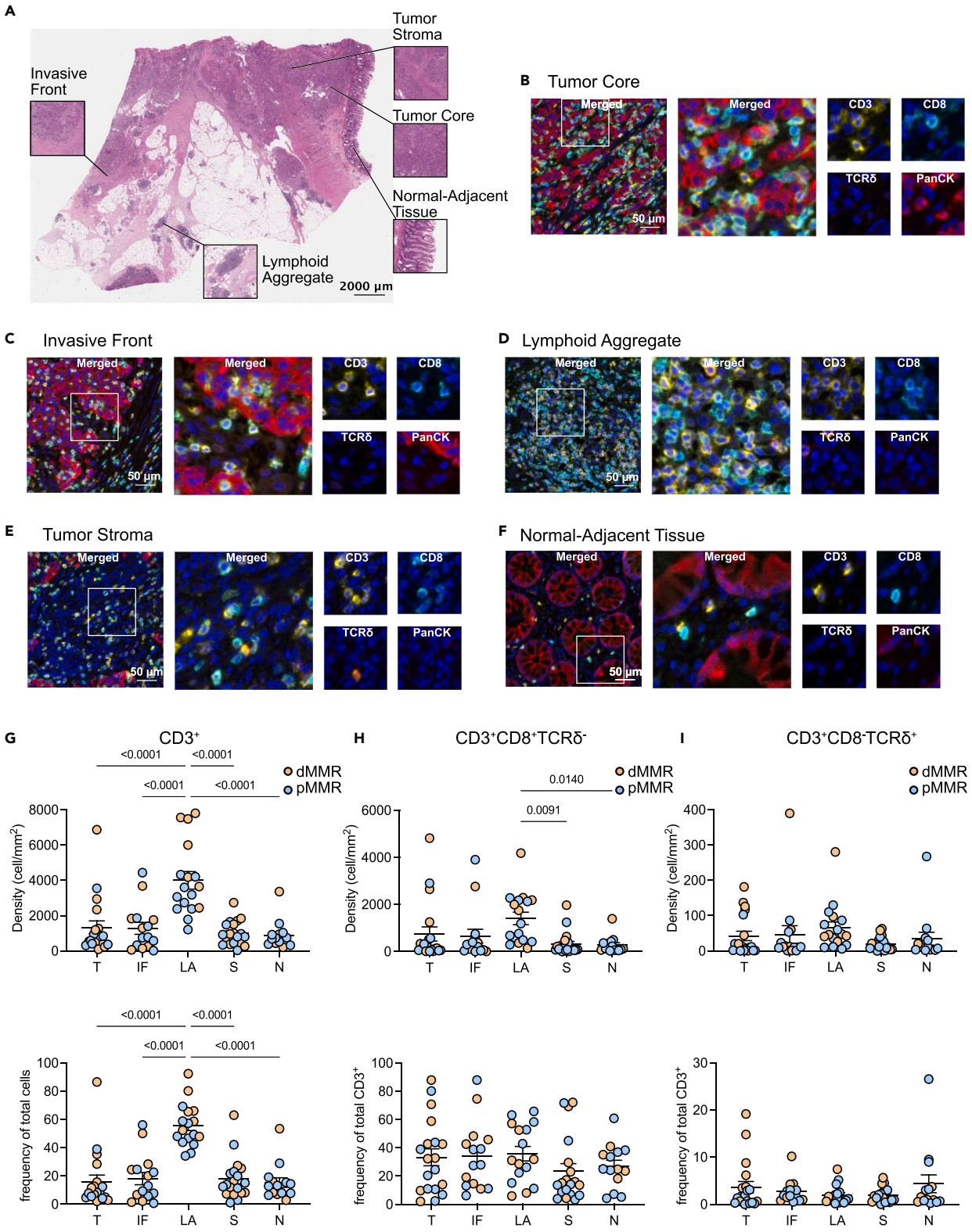

Figure 2. Differences in CD8$^+$ T cell and γδ T cell spatial distribution in stage III CRC

(A) Representative hematoxylin and eosin (H&E) staining of a stage III CRC tumor whole tissue section. Areas of interest for analysis include tumor stroma, tumor core, normal-adjacent tissue, lymphoid aggregates and invasive front. Scale bar: 2000 µm.

Figure 2. *Continued*

(B–F) Representative images of mIHC staining of the five compartments of interest, i.e., B) tumor core (T), C) invasive front (IF), D) lymphoid aggregate (LA), E) tumor stroma (S) and F) normal-adjacent tissue (N). Staining represented as merged and single channel staining for CD3, CD8, TCRδ and PanCK and are shown with DAPI staining. White square boxes are magnified to the right (middle panel). Scale bar: 50 μm.

(G–I) Densities (mm^2, upper panel) and frequencies (lower panel) of G) total $CD3^+$, H) $CD3^+CD8^+TCR\delta^-$ and I) $CD3^+CD8^-TCR\delta^+$ cells across the five tumor areas of interest. Orange data points show dMMR cases, blue data points show pMMR cases. Each point represents the average of five multispectral images per patient. Error bars represent SEMs. *p*-values calculated using one-way ANOVA test and only *p*-values < 0.05 are displayed.

staining showed that TCF-1^+ γδ T cells were more abundant in normal colon tissue adjacent to the tumor (Figure S2B left panel). Comparatively, TCF-1^- γδ T cells were equally abundant in all tumor areas analyzed (Figure S2B right panel). These results reveal that γδ T cells with reduced TCF-1 expression, that is linked to increased effector function, are differentially abundant in distinct regions of CRCs, with TCF-1^- effector γδ T cells present in all tumor regions, including the tumor core.

Abundance of TCF-1^+CD8^+ T cells is associated with improved survival in stage III CRC

Unlike γδ T cells, the role of TCF-1 in $CD8^+$ T cell differentiation has been intensely researched in recent years. $CD8^+$ T cell differentiation in tumors is complex, however recent reports have shown that under conditions of chronic stimulation, co-expression of TCF-1 and PD-1 marks a stem-like $CD8^+$ T cell population, known as T_{pex} cells. Due to their stem-like properties, T_{pex} cells are essential for maintaining $CD8^+$ T cell differentiation in response to ICI, and $CD8^+$TCF-1^+ T cells have been identified as an important predictor of clinical response to ICI in numerous cancer types.[39,41,43,44] Detailed investigation of TCF-1 expressing $CD8^+$ T cell subsets has not been previously examined in CRC. To begin, we set out to examine whether the presence of $CD8^+$TCF-1^+ T cells correlated with patient prognosis. We assessed tissue microarrays (TMAs) comprising colon tumors from 63 stage III patients, these were stained and analyzed using mIHC for CD3, CD8, TCF-1 and Pan Cytokeratin (PanCK) (Figure 3A). Analysis of $CD3^+CD8^+$TCF-1^+ tumor infiltrating T cells, revealed that the abundance of these cells correlated with improved disease-free (Figure 3B) and overall survival (Figure 3C). In contrast, total T cells or total $CD8^+$ T cells in this small patient cohort did not reveal significant association with patient outcome. Collectively, these results suggest that the abundance of $CD8^+$TCF-1^+ T cells could serve as a prognostic marker in CRC.

$CD8^+$TCF-1^+PD-1^+ Tpex cells are more abundant in lymphoid aggregates in stage III CRC

The experiments in Figure 3 analyzed total $CD8^+$TCF-1^+ T cells, the TMAs used contain only a small region of the total tumor, making it difficult to analyze smaller populations of cells including T_{pex} populations, and different structures, including lymphoid aggregates. Therefore, we next assessed $CD8^+$ T cell differentiation status in more detail within different tumor areas in both dMMR and pMMR tumors. $CD3^+CD8^+TCR\delta^-$ T cells were characterized according to their TCF-1 and PD-1 expression as follows; TCF-1^+PD-1^+ encompassing T_{pex} cells, TCF-1^-PD-1^+ cells that will contain subsets of T_{tex}, T_{eff} and early-exhausted populations, TCF-1^-PD-1^- that will contain T_{eff} cells and finally TCF-1^+PD-1^- containing naive or memory $CD8^+$ T cells. Representative $CD8^+$TCF-1^+PD-1^+ T_{pex} and $CD8^+$TCF-1^-PD-1^+ cell subsets located in lymphoid aggregates and tumor core, displayed positive staining for PD-1 (Figure 4A). Analysis of the frequency of each $CD3^+CD8^+TCR\delta^-$ subset revealed that $CD8^+$TCF-1^+PD-1^+ T_{pex} cells were significantly enriched in lymphoid aggregates compared to the tumor core and tumor stroma (Figure 4B). In contrast, the frequencies of $CD8^+$TCF-1^-PD-1^+ and $CD8^+$TCF-1^-PD-1^- cell subsets were similarly observed across all tumor areas, with the highest abundance in the tumor core (Figures 4C and 4D). Finally, $CD8^+$TCF-1^+PD-1^- naive or memory $CD8^+$ T cell subsets were enriched in lymphoid aggregates compared to other tumor regions (Figure 4E). Strikingly, similar frequencies of $CD8^+$TCF-1^+PD-1^+ T_{pex} cells and all other $CD3^+CD8^+TCR\delta^-$ cell subsets were observed in both TIL-hi dMMR and TIL-hi pMMR tumors. In some circumstances, including in lymph nodes, $CD8^+$TCF-1^+PD-1^+ T_{pex} cells have been shown to express the chemokine receptor CXCR5.[38,48,49] We observed CXCR5 expression on $CD8^+$ T cells in lymphoid aggregates of tumors from stage III CRC, but not in the tumor core (Figure S3A). Densities and the frequency of $CD3^+CD8^+CXCR5^+$ T cells were analyzed across the five tumor locations, which revealed these cells were primarily located in lymphoid aggregates, rather than any other tumor region (Figure S3B).

DISCUSSION

Surgery and chemotherapy have been the standard of care for non-mCRC patients for many years. However, relapse following treatment remains high at 20–40% for stage III CRC patients, and in some cases, treatment is associated with long term and serious side effects.[52] Therefore, more effective and safer treatment options are desperately needed to manage CRC. ICI has revolutionized the treatment of some cancer types, including melanoma and lung cancer. In CRC, ICI is currently used to treat patients with dMMR mCRC or dMMR rectal cancers.[9,23] ICI is yet to be widely used to treat early stage dMMR disease, however, recent clinical trials using ICI to treat dMMR and pMMR stage II and III CRC have demonstrated promising early results.[6,8–13] Although, more clinical trials with long-term outcome data and improved methods of tracking disease progression and treatment response are needed. We assessed $CD8^+$ T cell differentiation status, focusing on T_{pex} cells, which have recently been characterized as the major cell population responsible for reinvigorating T cell responses to promote tumor clearance following ICI.[2,38] Our analysis of $CD8^+$ T cell differentiation in stage III CRC elucidates patient populations with the presence of T_{pex} cells in lymphoid aggregates, indicating potential to respond to ICI.

Overall, we found that 24% of stage III CRC patients had robust TIL infiltration. A focused analysis of $CD8^+$ T cell differentiation revealed that $CD8^+$TCF-1^+PD-1^+ T_{pex} populations were present in tumors of stage III CRC patients and are specifically enriched in

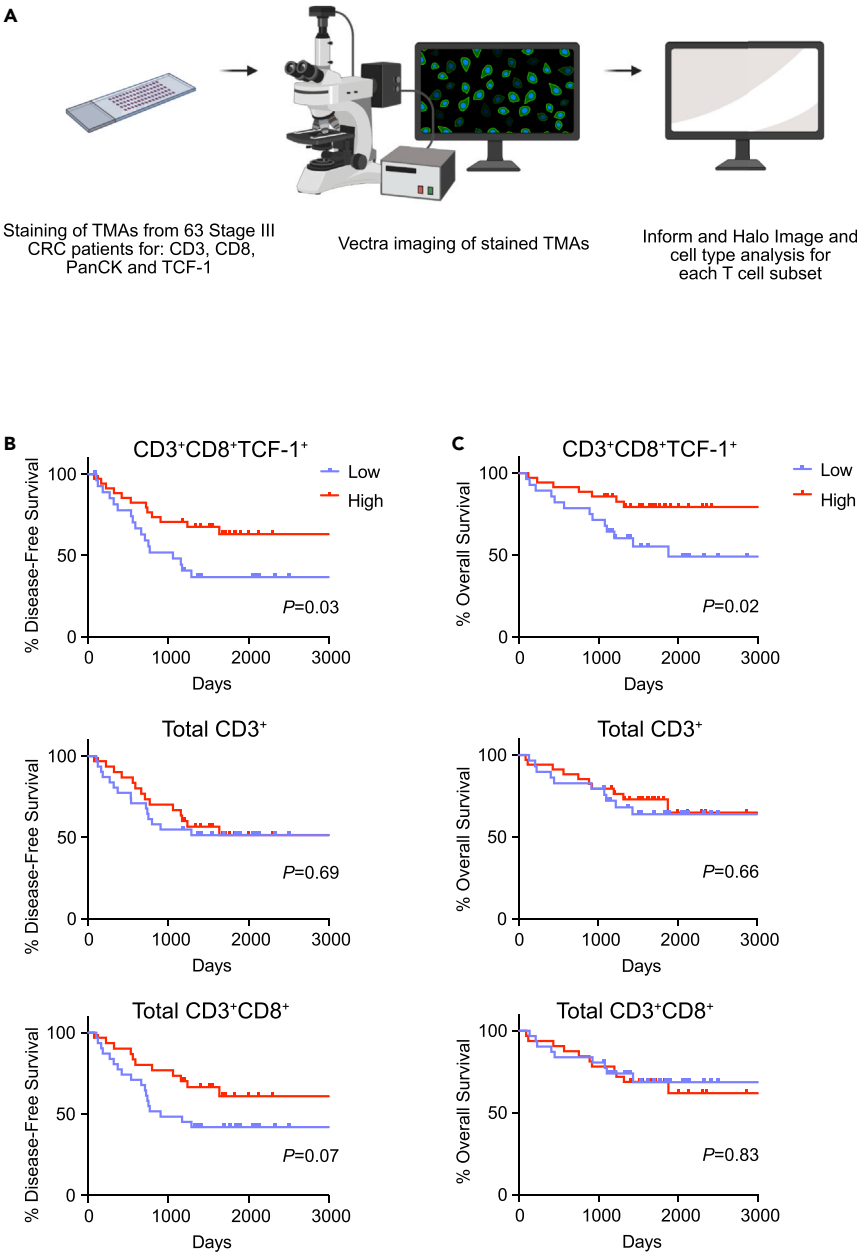

Figure 3. TCF-1-expressing CD8$^+$ T cells predict improved survival in stage III CRC

(A) Flowchart depicting overview of experiment setup.

(B and C) Percentage disease-free and C) overall survival of stage III CRC patients with high or low CD3$^+$CD8$^+$TCF-1$^+$, total CD3$^+$ or total CD3$^+$CD8$^+$ T cell infiltration. Staining and analysis is performed on 3 replicate tissue microarray samples per tumor from 63 stage III CRC patients. *p*-values calculated using Log rank Mantel-Cox test.

lymphoid aggregates, whereas CD8$^+$TCF-1$^-$PD-1$^+$ cells were most abundant in the tumor core and invasive tumor front. Little is known about the factors controlling recruitment, differentiation and maintenance of CD8$^+$TCF-1$^+$PD-1$^+$ T_{pex} cells in colon tumors. An important relationship between dendritic cells (DCs) and T_{pex} cells is emerging. T_{pex} cells have the potential to secrete XCL1, which is important for dendritic cell recruitment. Analysis of lung, kidney, bladder and prostate cancers showed DCs co-reside with T_{pex} cells within distinct anatomical niches.[42] Two recent studies further interrogated the localization of DCs with T_{pex} cells within intratumoral "lymphonets" or "immunity hubs" that are abundant in early-stage human lung adenocarcinoma.[45,46] These structures are often less organized and lack distinct T and B cell zones compared with tertiary lymphoid structures. These finding are consistent with our results showing that CD8$^+$TCF-1$^+$PD-1$^+$ T_{pex} cells are largely restricted to lymphoid aggregates and these

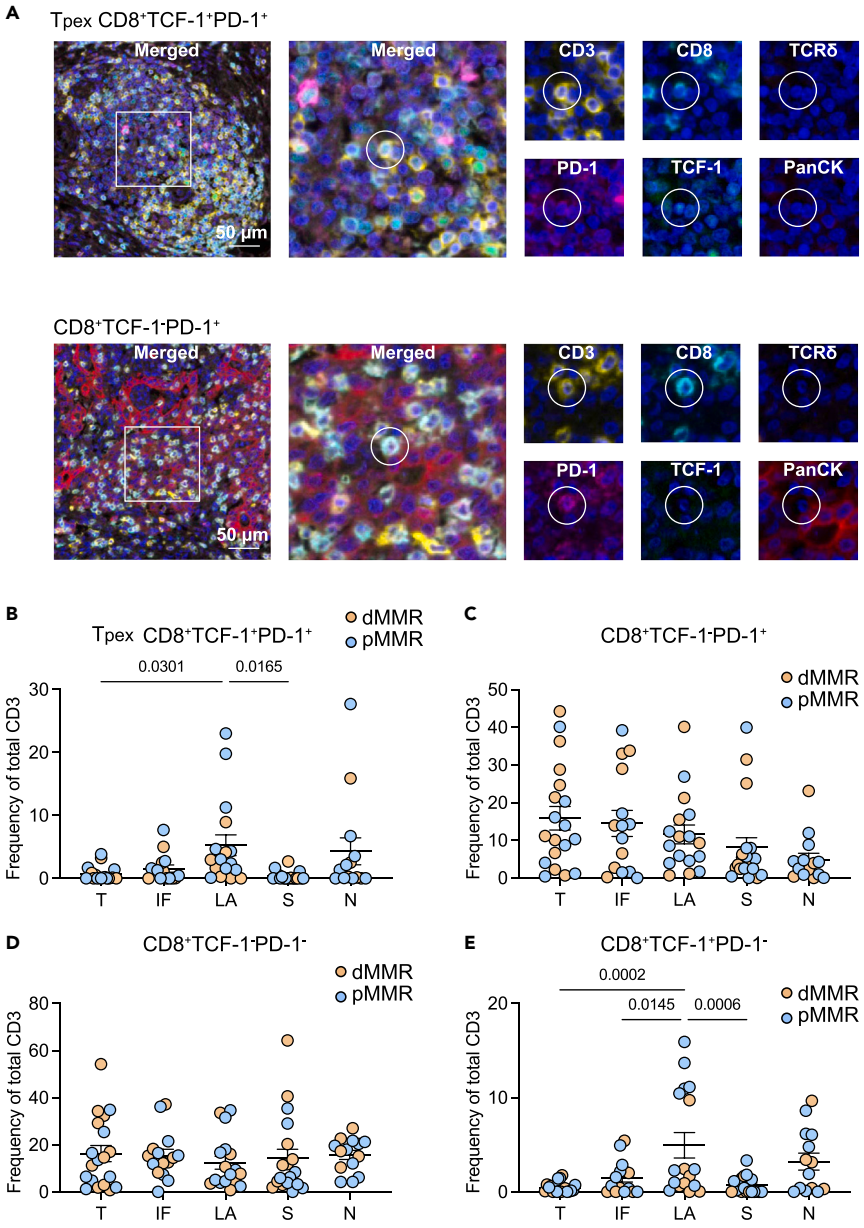

Figure 4. CD8$^+$TCF-1$^+$PD-1$^+$ T_{pex} cells are more abundant in lymphoid aggregates in stage III CRC

(A) Representative CD8$^+$TCF-1$^+$PD-1$^+$ T_{pex} (upper panel) and CD8$^+$TCF-1$^-$PD-1$^+$ T cells (lower panel) mIHC staining in a lymphoid aggregate and tumor core of stage III CRC whole tumor section. Merged images display overlay of CD3, CD8, TCRδ, PD-1, TCF-1, PanCK and DAPI staining. Single stains of CD3, CD8, TCRδ, PD-1, TCF-1 and PanCK are shown with DAPI staining. White square boxes are magnified to the right (middle panel). Scale bar: 50 μm.

(B–E) Percentage frequencies of B) T_{pex} (CD8$^+$TCF-1$^+$PD-1$^+$), C) CD8$^+$TCF-1$^-$PD-1$^+$, D) CD8$^+$TCF-1$^-$PD-1$^-$ and E) CD8$^+$TCF-1$^+$PD-1$^-$ T cell subsets across the five tumor areas of interest; tumor core (T), invasive front (IF), lymphoid aggregates (LA), tumor stroma (S) and normal-adjacent tissue (N). Percentage frequencies for each CD8$^+$ T cell subset is calculated based on the total CD3$^+$ T cell count. Orange data points represent dMMR cases, blue data points represent pMMR cases. Each point represents the average of five multispectral images per patient. Error bars represent SEMs. *p*-values calculated using one-way ANOVA test and only *p*-values < 0.05 are shown.

findings are consistent across tumor types. In addition, in mouse models of lung cancer, migratory type 1 conventional DCs (cDC1) facilitated the recruitment and maintenance of T_{pex} cells within the lung and the draining lymph node.[53,54] Further studies investigating T_{pex} development within the tumor and intestinal microenvironment, will be essential to elucidate new opportunities to exploit these cells and maintain robust immune responses in defense against CRC.

Our analysis focused on TIL-hi CRCs and in this cohort revealed no significant differences in T_{pex} cell differentiation, including $CD8^+TCF\text{-}1^+PD\text{-}1^+$ T_{pex} frequency between the dMMR and pMMR patient cohorts. Our selection of TIL-hi cases provides a unique outlook of the CRC landscape providing evidence that some TIL-high pMMR patients can exert $CD8^+$ T cell responses that could be comparable to patients with dMMR tumors. These results in combination with recent clinical trials[3,6] and reports showing that high immune cell infiltration is superior to MMR status in predicting CRC patient survival outcomes,[19,21] raises an emerging hypothesis for the field, that additional cohorts of CRC patients may respond to ICI.

In addition to our analysis of $CD8^+$ T cell differentiation, we also investigated spatial distribution of γδ T cells. Unlike $CD8^+$ T cell subsets, the γδ T cells were evenly distributed throughout the tumor microenvironment. In agreement with our previous study, $TCF\text{-}1^+$ γδ T cells were most abundant in normal colon epithelium compared with tumor areas. TCF-1 acts to suppress colon γδ T cell anti-tumor defense and effector functions, limiting molecules important for DC recruitment and cytotoxicity, including XCL1 and Granzyme B.[28] The role of PD-1 on colon γδ T cells is beginning to emerge, its expression has been associated with tumor reactive colon γδ T cells,[25] however much more work is needed to determine the function of PD-1 and other checkpoint receptors on colon γδ T cells and how they influence the anti-tumor defense of the two major human γδ T cell subsets, Vδ1 and Vδ2 in tissues and circulation. Overall, our data reveals differences in $CD8^+$ T cell and γδ T cell spatial distribution in stage III CRC, highlighting the importance of analyzing immune responses in lymphoid aggregates in addition to the tumor core. Further studies investigating factors regulating development of lymphoid aggregates in CRC, may provide insights for future immunotherapy strategies[55] and provide opportunities to exploit T_{pex} differentiation or identify new biomarkers to predict treatment response in CRC.

Limitations of the study

The aim of this study was to investigate T cell differentiation in TIL-hi stage III CRC and compare T cell differentiation between the two major disease subtypes, dMMR and pMMR CRC. We found that in a subgroup of stage III CRCs with high TIL infiltration, the presence of $CD3^+CD8^+TCF\text{-}1^+$ T cells predicted improved survival of patients and $CD3^+CD8^+TCF\text{-}1^+PD\text{-}1^+$ T_{pex} cells were enriched in lymphoid aggregates in both subtypes of dMMR and pMMR TIL-hi tumors. However, there are a number of limitations with our study and further investigation of T cell differentiation in CRC will shed light on the role of $CD8^+$ T cells in CRC and whether they can be harnessed with immunotherapies to benefit patients. Limitations include the TIL scoring method used; only lymphocytes infiltrating the tumor epithelium are counted to generate the TIL score, however, other TIL or immune scoring protocols exist and future comparison of these different methods would be useful to determine effective methods to predict patient outcomes.[56] In addition, our analyses of T cell differentiation in different tumor regions highlight lymphoid aggregates as a region of interest; however, very recent reports describe similar regions of interest and a future comprehensive analysis of these structures in comparison to tertiary lymphoid structures should be performed. Finally, increasing patient numbers in the analysis and the inclusion of additional markers of exhaustion and T cell activation, including TIM3 and Granzyme B, would allow us to confirm our findings in independent patient cohorts and more accurately distinguish exhausted and effector $CD8^+$ T cell subsets in CRC. Increasing the patient cohort will also allow us to better correlate the number of T_{pex} cells with MMR or TIL status in association with patient survival. Currently, this is not possible with the small sample size.

RESOURCE AVAILABILITY

Lead contact

Further information and requests for resources and reagents should be directed to and will be fulfilled by the lead contact, L.A.M. (lisa.mielke@onjcri.org.au).

Materials availability

This study did not generate new unique reagents.

Data and code availability

Data reported in this paper will be shared by the lead contact upon request. This paper does not report original code. Any additional information required to reanalyze the data reported in this paper is available from the lead contact upon request.

ACKNOWLEDGMENTS

We thank our consumers and patient advocates for their advice, patients and their families who donated human tissues for use in this study and the Austin Hospital ethics committee for their guidance. We thank the Victorian Cancer Biobank through the Cancer Council Victoria as Lead Agency is supported by the Victorian Government through the Victorian Cancer Agency, a business unit of the Department of Health. This research was funded by The Australian National Health and Medical Research Council Ideas Grants 2011558 (L.A.M.) and 1185513 (L.A.M. and D.W.), Victorian Cancer Agency mid-career and early career fellowships (L.A.M. and D.R.), Cure Cancer Australia, Priority Driven Young Investigator Grant 1123388 (L.A.M.) and Veski Career Recovery Grant (L.A.M.).

AUTHOR CONTRIBUTIONS

Investigation: K.T., A.N.K., D.R., D.S.W., and L.A.M. Resources: D.S.W. and A.B. Supervision: L.A.M., D.S.W., V.M., D.R.A.C., S.K.G., M.V.P., J.M., and N.C.T. Funding acquisition: L.A.M., D.S.W., D.R., and N.C.T. Writing original draft: K.T. and L.A.M. Conceptualization: L.A.M.

DECLARATION OF INTERESTS

The authors declare no competing interests.

STAR★METHODS

Detailed methods are provided in the online version of this paper and include the following:

- KEY RESOURCES TABLE
- EXPERIMENTAL MODEL AND STUDY PARTICIPANT DETAILS STUDY PARTICIPANTS
- METHOD DETAILS
  - Multiplex immunohistochemistry (IHC)
  - Imaging and analysis
- QUANTIFICATION AND STATISTICAL ANALYSIS

SUPPLEMENTAL INFORMATION

Supplemental information can be found online at https://doi.org/10.1016/j.isci.2024.110754.

Received: December 27, 2023
Revised: March 11, 2024
Accepted: August 13, 2024
Published: August 22, 2024

REFERENCES

1. Sung, H., Ferlay, J., Siegel, R.L., Laversanne, M., Soerjomataram, I., Jemal, A., and Bray, F. (2021). Global Cancer Statistics 2020: GLOBOCAN Estimates of Incidence and Mortality Worldwide for 36 Cancers in 185 Countries. CA A Cancer J. Clin. *71*, 209–249. https://doi.org/10.3322/caac.21660.
2. Zehn, D., Thimme, R., Lugli, E., de Almeida, G.P., and Oxenius, A. (2022). 'Stem-like' precursors are the fount to sustain persistent CD8(+) T cell responses. Nat. Immunol. *23*, 836–847. https://doi.org/10.1038/s41590-022-01219-w.
3. Ozer, M., Vegivinti, C.T.R., Syed, M., Ferrell, M.E., Gonzalez Gomez, C., Cheng, S., Holder-Murray, J., Bruno, T., Saeed, A., and Sahin, I.H. (2023). Neoadjuvant Immunotherapy for Patients with dMMR/MSI-High Gastrointestinal Cancers: A Changing Paradigm. Cancers *15*, 3833. https://doi.org/10.3390/cancers15153833.
4. Huyghe, N., Baldin, P., and Van den Eynde, M. (2020). Immunotherapy with immune checkpoint inhibitors in colorectal cancer: what is the future beyond deficient mismatch-repair tumours? Gastroenterol. Rep. *8*, 11–24. https://doi.org/10.1093/gastro/goz061.
5. Kreidieh, M., Mukherji, D., Temraz, S., and Shamseddine, A. (2020). Expanding the Scope of Immunotherapy in Colorectal Cancer: Current Clinical Approaches and Future Directions. BioMed Res. Int. *2020*, 9037217. https://doi.org/10.1155/2020/9037217.
6. Chalabi, M., Fanchi, L.F., Dijkstra, K.K., Van den Berg, J.G., Aalbers, A.G., Sikorska, K., Lopez-Yurda, M., Grootscholten, C., Beets, G.L., Snaebjornsson, P., et al. (2020). Neoadjuvant immunotherapy leads to pathological responses in MMR-proficient and MMR-deficient early-stage colon cancers. Nat. Med. *26*, 566–576. https://doi.org/10.1038/s41591-020-0805-8.
7. Saude-Conde, R., Nguyen, D., and Hendlisz, A. (2023). Immunotherapies in non-metastatic gastrointestinal cancers. Curr. Opin. Oncol. *35*, 334–346. https://doi.org/10.1097/CCO.0000000000000956.
8. Barraud, S., Tougeron, D., Villeneuve, L., Eveno, C., Bayle, A., Parc, Y., Pocard, M., André, T., and Cohen, R. (2023). Immune checkpoint inhibitors for patients with isolated peritoneal carcinomatosis from dMMR/MSI-H colorectal cancer, a BIG-RENAPE collaboration. Dig. Liver Dis. *55*, 673–678. https://doi.org/10.1016/j.dld.2022.09.015.
9. Cercek, A., Lumish, M., Sinopoli, J., Weiss, J., Shia, J., Lamendola-Essel, M., El Dika, I.H., Segal, N., Shcherba, M., Sugarman, R., et al. (2022). PD-1 Blockade in Mismatch Repair-Deficient, Locally Advanced Rectal Cancer. N. Engl. J. Med. *386*, 2363–2376. https://doi.org/10.1056/NEJMoa2201445.
10. Ludford, K., Ho, W.J., Thomas, J.V., Raghav, K.P.S., Murphy, M.B., Fleming, N.D., Lee, M.S., Smaglo, B.G., You, Y.N., Tillman, M.M., et al. (2023). Neoadjuvant Pembrolizumab in Localized Microsatellite Instability High/Deficient Mismatch Repair Solid Tumors. J. Clin. Oncol. *41*, 2181–2190. https://doi.org/10.1200/JCO.22.01351.
11. Zhang, X., Yang, R., Wu, T., Cai, X., Li, G., Yu, K., Li, Y., Ding, R., Dong, C., Li, J., et al. (2022). Efficacy and Safety of Neoadjuvant Monoimmunotherapy With PD-1 Inhibitor for dMMR/MSI rectangleH Locally Advanced Colorectal Cancer: A Single-Center Real-World Study. Front. Immunol. *13*, 913483. https://doi.org/10.3389/fimmu.2022.913483.
12. Wang, Q., Xiao, B., Jiang, W., Steele, S., Cai, J., Pan, Z., Zhang, X., and Ding, P. (2021). P-187 Watch-and-wait strategy for DNA mismatch repair-deficient/microsatellite instability-high rectal cancer with a clinical complete response after neoadjuvant immunotherapy: An observational cohort study. Ann. Oncol. *32*, S163–S164. https://doi.org/10.1016/j.annonc.2021.05.242.
13. Chalabi, M., Verschoor, Y., van den Berg, J., Sikorska, K., Beets, G., Lent, A., Grootscholten, M., Aalbers, A., Buller, N., Marsman, H., et al. (2022). LBA7 Neoadjuvant immune checkpoint inhibition in locally advanced MMR-deficient colon cancer: The NICHE-2 study. Ann. Oncol. *33*, S1389. https://doi.org/10.1016/j.annonc.2022.08.016.
14. Pei, F., Wu, J., Zhao, Y., He, W., Yao, Q., Huang, M., and Huang, J. (2023). Single-Agent Neoadjuvant Immunotherapy With a PD-1 Antibody in Locally Advanced Mismatch Repair-Deficient or Microsatellite Instability-High Colorectal Cancer. Clin. Colorectal Cancer *22*, 85–91. https://doi.org/10.1016/j.clcc.2022.11.004.
15. Chalabi, M., Verschoor, Y.L., Tan, P.B., Balduzzi, S., Van Lent, A.U., Grootscholten, C., Dokter, S., Büller, N.V., Grotenhuis, B.A., Kuhlmann, K., et al. (2024). Neoadjuvant Immunotherapy in Locally Advanced Mismatch Repair-Deficient Colon Cancer. N. Engl. J. Med. *390*, 1949–1958. https://doi.org/10.1056/NEJMoa2400634.
16. Kim, J.H., Kim, K.J., Bae, J.M., Rhee, Y.Y., Cho, N.Y., Lee, H.S., and Kang, G.H. (2015). Comparative validation of assessment criteria for Crohn-like lymphoid reaction in colorectal carcinoma. J. Clin. Pathol. *68*, 22–28. https://doi.org/10.1136/jclinpath-2014-202603.
17. Maoz, A., Dennis, M., and Greenson, J.K. (2019). The Crohn's-Like Lymphoid Reaction to Colorectal Cancer-Tertiary Lymphoid Structures With Immunologic and Potentially Therapeutic Relevance in Colorectal Cancer. Front. Immunol. *10*, 1884. https://doi.org/10.3389/fimmu.2019.01884.
18. Rozek, L.S., Schmit, S.L., Greenson, J.K., Tomsho, L.P., Rennert, H.S., Rennert, G., and Gruber, S.B. (2016). Tumor-Infiltrating Lymphocytes, Crohn's-Like Lymphoid Reaction, and Survival From Colorectal Cancer. J. Natl. Cancer Inst. *108*, djw027. https://doi.org/10.1093/jnci/djw027.
19. Williams, D.S., Mouradov, D., Jorissen, R.N., Newman, M.R., Amini, E., Nickless, D.K., Teague, J.A., Fang, C.G., Palmieri, M., Parsons, M.J., et al. (2019). Lymphocytic response to tumour and deficient DNA mismatch repair identify subtypes of stage II/III colorectal cancer associated with patient outcomes. Gut *68*, 465–474. https://doi.org/10.1136/gutjnl-2017-315664.
20. Fuchs, T.L., Sioson, L., Sheen, A., Jafari-Nejad, K., Renaud, C.J., Andrici, J., Ahadi, M.,

Chou, A., and Gill, A.J. (2020). Assessment of Tumor-infiltrating Lymphocytes Using International TILs Working Group (ITWG) System Is a Strong Predictor of Overall Survival in Colorectal Carcinoma: A Study of 1034 Patients. Am. J. Surg. Pathol. *44*, 536–544. https://doi.org/10.1097/PAS.0000000000001409.

21. Mlecnik, B., Bindea, G., Angell, H.K., Maby, P., Angelova, M., Tougeron, D., Church, S.E., Lafontaine, L., Fischer, M., Fredriksen, T., et al. (2016). Integrative Analyses of Colorectal Cancer Show Immunoscore Is a Stronger Predictor of Patient Survival Than Microsatellite Instability. Immunity *44*, 698–711. https://doi.org/10.1016/j.immuni.2016.02.025.
22. Williams, D.S., Mouradov, D., Newman, M.R., Amini, E., Nickless, D.K., Fang, C.G., Palmieri, M., Sakthianandeswaren, A., Li, S., Ward, R.L., et al. (2020). Tumour infiltrating lymphocyte status is superior to histological grade, DNA mismatch repair and BRAF mutation for prognosis of colorectal adenocarcinomas with mucinous differentiation. Mod. Pathol. *33*, 1420–1432. https://doi.org/10.1038/s41379-020-0496-1.
23. Loupakis, F., Depetris, I., Biason, P., Intini, R., Prete, A.A., Leone, F., Lombardi, P., Filippi, R., Spallanzani, A., Cascinu, S., et al. (2020). Prediction of Benefit from Checkpoint Inhibitors in Mismatch Repair Deficient Metastatic Colorectal Cancer: Role of Tumor Infiltrating Lymphocytes. Oncol. *25*, 481–487. https://doi.org/10.1634/theoncologist.2019-0611.
24. Le, D.T., Uram, J.N., Wang, H., Bartlett, B.R., Kemberling, H., Eyring, A.D., Skora, A.D., Luber, B.S., Azad, N.S., Laheru, D., et al. (2015). PD-1 Blockade in Tumors with Mismatch-Repair Deficiency. N. Engl. J. Med. *372*, 2509–2520. https://doi.org/10.1056/NEJMoa1500596.
25. de Vries, N.L., van de Haar, J., Veninga, V., Chalabi, M., Ijsselsteijn, M.E., van der Ploeg, M., van den Bulk, J., Ruano, D., van den Berg, J.G., Haanen, J.B., et al. (2023). gammadelta T cells are effectors of immunotherapy in cancers with HLA class I defects. Nature *613*, 743–750. https://doi.org/10.1038/s41586-022-05593-1.
26. Galon, J., Costes, A., Sanchez-Cabo, F., Kirilovsky, A., Mlecnik, B., Lagorce-Pagès, C., Tosolini, M., Camus, M., Berger, A., Wind, P., et al. (2006). Type, density, and location of immune cells within human colorectal tumors predict clinical outcome. Science *313*, 1960–1964. https://doi.org/10.1126/science.1129139.
27. Gentles, A.J., Newman, A.M., Liu, C.L., Bratman, S.V., Feng, W., Kim, D., Nair, V.S., Xu, Y., Khuong, A., Hoang, C.D., et al. (2015). The prognostic landscape of genes and infiltrating immune cells across human cancers. Nat. Med. *21*, 938–945. https://doi.org/10.1038/nm.3909.
28. Yakou, M.H., Ghilas, S., Tran, K., Liao, Y., Afshar-Sterle, S., Kumari, A., Schmid, K., Dijkstra, C., Inguanti, C., Ostrouska, S., et al. (2023). TCF-1 limits intraepithelial lymphocyte antitumor immunity in colorectal carcinoma. Sci. Immunol. *8*, eadf2163. https://doi.org/10.1126/sciimmunol.adf2163.
29. Mikulak, J., Oriolo, F., Bruni, E., Roberto, A., Colombo, F.S., Villa, A., Bosticardo, M., Bortolomai, I., Lo Presti, E., Meraviglia, S., et al. (2019). NKp46-expressing human gut-resident intraepithelial Vdelta1 T cell subpopulation exhibits high antitumor activity against colorectal cancer. JCI Insight *4*, e125884. https://doi.org/10.1172/jci.insight.125884.
30. Reis, B.S., Darcy, P.W., Khan, I.Z., Moon, C.S., Kornberg, A.E., Schneider, V.S., Alvarez, Y., Eleso, O., Zhu, C., Schernthanner, M., et al. (2022). TCR-Vgammadelta usage distinguishes protumor from antitumor intestinal gammadelta T cell subsets. Science *377*, 276–284. https://doi.org/10.1126/science.abj8695.
31. Meraviglia, S., Lo Presti, E., Tosolini, M., La Mendola, C., Orlando, V., Todaro, M., Catalano, V., Stassi, G., Cicero, G., Vieni, S., et al. (2017). Distinctive features of tumor-infiltrating gammadelta T lymphocytes in human colorectal cancer. OncoImmunology *6*, e1347742. https://doi.org/10.1080/2162402X.2017.1347742.
32. Morikawa, R., Nemoto, Y., Yonemoto, Y., Tanaka, S., Takei, Y., Oshima, S., Nagaishi, T., Tsuchiya, K., Nozaki, K., Mizutani, T., et al. (2021). Intraepithelial Lymphocytes Suppress Intestinal Tumor Growth by Cell-to-Cell Contact via CD103/E-Cadherin Signal. Cell. Mol. Gastroenterol. Hepatol. *11*, 1483–1503. https://doi.org/10.1016/j.jcmgh.2021.01.014.
33. Suzuki, T., Kilbey, A., Casa-Rodriguez, N., Lawlor, A., Georgakopoulou, A., Hayman, H., Yin Swe, K.L., Nordin, A., Cantu, C., Vantourout, P., et al. (2023). beta-Catenin Drives Butyrophilin-like Molecule Loss and gammadelta T-cell Exclusion in Colon Cancer. Cancer Immunol. Res. *11*, 1137–1155. https://doi.org/10.1158/2326-6066.CIR-22-0644.
34. Rancan, C., Arias-Badia, M., Dogra, P., Chen, B., Aran, D., Yang, H., Luong, D., Ilano, A., Li, J., Chang, H., et al. (2023). Exhausted intratumoral Vdelta2(-) gammadelta T cells in human kidney cancer retain effector function. Nat. Immunol. *24*, 612–624. https://doi.org/10.1038/s41590-023-01448-7.
35. He, R., Hou, S., Liu, C., Zhang, A., Bai, Q., Han, M., Yang, Y., Wei, G., Shen, T., Yang, X., et al. (2016). Follicular CXCR5- expressing CD8(+) T cells curtail chronic viral infection. Nature *537*, 412–428. https://doi.org/10.1038/nature19317.
36. Im, S.J., Hashimoto, M., Gerner, M.Y., Lee, J., Kissick, H.T., Burger, M.C., Shan, Q., Hale, J.S., Lee, J., Nasti, T.H., et al. (2016). Defining CD8+ T cells that provide the proliferative burst after PD-1 therapy. Nature *537*, 417–421. https://doi.org/10.1038/nature19330.
37. Utzschneider, D.T., Charmoy, M., Chennupati, V., Pousse, L., Ferreira, D.P., Calderon-Copete, S., Danilo, M., Alfei, F., Hofmann, M., Wieland, D., et al. (2016). T Cell Factor 1-Expressing Memory-like CD8(+) T Cells Sustain the Immune Response to Chronic Viral Infections. Immunity *45*, 415–427. https://doi.org/10.1016/j.immuni.2016.07.021.
38. Raghu, D., Xue, H.H., and Mielke, L.A. (2019). Control of Lymphocyte Fate, Infection, and Tumor Immunity by TCF-1. Trends Immunol. *40*, 1149–1162. https://doi.org/10.1016/j.it.2019.10.006.
39. Sade-Feldman, M., Yizhak, K., Bjorgaard, S.L., Ray, J.P., de Boer, C.G., Jenkins, R.W., Lieb, D.J., Chen, J.H., Frederick, D.T., Barzily-Rokni, M., et al. (2018). Defining T Cell States Associated with Response to Checkpoint Immunotherapy in Melanoma. Cell *175*, 998–1013.e20. https://doi.org/10.1016/j.cell.2018.10.038.
40. Brummelman, J., Mazza, E.M.C., Alvisi, G., Colombo, F.S., Grilli, A., Mikulak, J., Mavilio, D., Alloisio, M., Ferrari, F., Lopci, E., et al. (2018). High-dimensional single cell analysis identifies stem-like cytotoxic CD8(+) T cells infiltrating human tumors. J. Exp. Med. *215*, 2520–2535. https://doi.org/10.1084/jem.20180684.
41. Gettinger, S.N., Choi, J., Mani, N., Sanmamed, M.F., Datar, I., Sowell, R., Du, V.Y., Kaftan, E., Goldberg, S., Dong, W., et al. (2018). A dormant TIL phenotype defines non-small cell lung carcinomas sensitive to immune checkpoint blockers. Nat. Commun. *9*, 3196. https://doi.org/10.1038/s41467-018-05032-8.
42. Jansen, C.S., Prokhnevska, N., Master, V.A., Sanda, M.G., Carlisle, J.W., Bilen, M.A., Cardenas, M., Wilkinson, S., Lake, R., Sowalsky, A.G., et al. (2019). An intra-tumoral niche maintains and differentiates stem-like CD8 T cells. Nature *576*, 465–470. https://doi.org/10.1038/s41586-019-1836-5.
43. Miller, B.C., Sen, D.R., Al Abosy, R., Bi, K., Virkud, Y.V., LaFleur, M.W., Yates, K.B., Lako, A., Felt, K., Naik, G.S., et al. (2019). Subsets of exhausted CD8(+) T cells differentially mediate tumor control and respond to checkpoint blockade. Nat. Immunol. *20*, 326–336. https://doi.org/10.1038/s41590-019-0312-6.
44. Siddiqui, I., Schaeuble, K., Chennupati, V., Fuertes Marraco, S.A., Calderon-Copete, S., Pais Ferreira, D., Carmona, S.J., Scarpellino, L., Gfeller, D., Pradervand, S., et al. (2019). Intratumoral Tcf1(+)PD-1(+)CD8(+) T Cells with Stem-like Properties Promote Tumor Control in Response to Vaccination and Checkpoint Blockade Immunotherapy. Immunity *50*, 195–211.e10. https://doi.org/10.1016/j.immuni.2018.12.021.
45. Chen, J.H., Nieman, L.T., Spurrell, M., Jorgji, V., Elmelech, L., Richieri, P., Xu, K.H., Madhu, R., Parikh, M., Zamora, I., et al. (2024). Human lung cancer harbors spatially organized stem-immunity hubs associated with response to immunotherapy. Nat. Immunol. *25*, 644–658. https://doi.org/10.1038/s41590-024-01792-2.
46. Gaglia, G., Burger, M.L., Ritch, C.C., Rammos, D., Dai, Y., Crossland, G.E., Tavana, S.Z., Warchol, S., Jaeger, A.M., Naranjo, S., et al. (2023). Lymphocyte networks are dynamic cellular communities in the immunoregulatory landscape of lung adenocarcinoma. Cancer Cell *41*, 871–886.e10. https://doi.org/10.1016/j.ccell.2023.03.015.
47. Im, S.J., Obeng, R.C., Nasti, T.H., McManus, D., Kamphorst, A.O., Gunisetty, S., Prokhnevska, N., Carlisle, J.W., Yu, K., Sica, G.L., et al. (2023). Characteristics and anatomic location of PD-1(+)TCF1(+) stem-like CD8 T cells in chronic viral infection and cancer. Proc. Natl. Acad. Sci. USA *120*, e2221985120. https://doi.org/10.1073/pnas.2221985120.
48. E, J., Yan, F., Kang, Z., Zhu, L., Xing, J., and Yu, E. (2018). CD8(+)CXCR5(+) T cells in tumor-draining lymph nodes are highly activated and predict better prognosis in colorectal cancer. Hum. Immunol. *79*, 446–452. https://doi.org/10.1016/j.humimm.2018.03.003.
49. Xing, J., Zhang, C., Yang, X., Wang, S., Wang, Z., Li, X., and Yu, E. (2017). CXCR5(+)CD8(+) T cells infiltrate the colorectal tumors and nearby lymph nodes, and are associated with enhanced IgG response in B cells. Exp. Cell

Res. *356*, 57–63. https://doi.org/10.1016/j.yexcr.2017.04.014.

50. de Vries, N.L., van Unen, V., Ijsselsteijn, M.E., Abdelaal, T., van der Breggen, R., Farina Sarasqueta, A., Mahfouz, A., Peeters, K.C.M.J., Höllt, T., Lelieveldt, B.P.F., et al. (2020). High-dimensional cytometric analysis of colorectal cancer reveals novel mediators of antitumour immunity. Gut *69*, 691–703. https://doi.org/10.1136/gutjnl-2019-318672.
51. Edwards, S.C., Hedley, A., Hoevenaar, W.H.M., Wiesheu, R., Glauner, T., Kilbey, A., Shaw, R., Boufea, K., Batada, N., Hatano, S., et al. (2023). PD-1 and TIM-3 differentially regulate subsets of mouse IL-17A-producing gammadelta T cells. J. Exp. Med. *220*, e20211431. https://doi.org/10.1084/jem.20211431.
52. Grothey, A., Sobrero, A.F., Shields, A.F., Yoshino, T., Paul, J., Taieb, J., Souglakos, J., Shi, Q., Kerr, R., Labianca, R., et al. (2018). Duration of Adjuvant Chemotherapy for Stage III Colon Cancer. N. Engl. J. Med. *378*, 1177–1188. https://doi.org/10.1056/NEJMoa1713709.
53. Ghilas, S., and Mielke, L.A. (2021). Dendritic cells shape TCF1(+)CD8(+) progenitor T cell heterogeneity. Trends Immunol. *42*, 1063–1065. https://doi.org/10.1016/j.it.2021.10.013.
54. Schenkel, J.M., Herbst, R.H., Canner, D., Li, A., Hillman, M., Shanahan, S.L., Gibbons, G., Smith, O.C., Kim, J.Y., Westcott, P., et al. (2021). Conventional type I dendritic cells maintain a reservoir of proliferative tumor-antigen specific TCF-1(+) CD8(+) T cells in tumor-draining lymph nodes. Immunity *54*, 2338–2353.e6. https://doi.org/10.1016/j.immuni.2021.08.026.
55. Zhang, Y., Xu, M., Ren, Y., Ba, Y., Liu, S., Zuo, A., Xu, H., Weng, S., Han, X., and Liu, Z. (2024). Tertiary lymphoid structural heterogeneity determines tumour immunity and prospects for clinical application. Mol. Cancer *23*, 75. https://doi.org/10.1186/s12943-024-01980-6.
56. Moretto, R., Rossini, D., Catteau, A., Antoniotti, C., Giordano, M., Boccaccino, A., Ugolini, C., Proietti, A., Conca, V., Kassambara, A., et al. (2023). Dissecting tumor lymphocyte infiltration to predict benefit from immune-checkpoint inhibitors in metastatic colorectal cancer: lessons from the AtezoT RIBE study. J. Immunother. Cancer *11*, e006633. https://doi.org/10.1136/jitc-2022-006633.

STAR★METHODS

KEY RESOURCES TABLE

REAGENT or RESOURCE	SOURCE	IDENTIFIER
Antibodies		
CD3 [SP7]	Abcam	Cat #: AB16669; RRID: AB_443425
CD8 [4B11]	GeneTex	Cat #: GTX75394; RRID: AB_376778
CXCR5 [Polyclonal]	Atlas Antibodies	Cat #: HPA042432; RRID: AB_2677995
PanCK [AE1/AE7]	Leica Biosystems	Cat #: PA0094
PD-1 [NAT105]	Abcam	Cat #: AB52587; RRID: AB_881954
TCF-1 [C63D9]	Cell Signaling Technology	Cat #: 2203S
TCRδ [H-41]	Santa Cruz Biotechnology	Cat #: SC-100289; RRID: AB_1130061
Biological samples		
All Stage III CRC primary tumor samples were retrospectively collected from patients recruited at Austin Health from Austin pathology or from Victorian Cancer Biobank	Austin Pathology or Victorian Cancer Biobank	
Critical commercial assays		
Opal 7-Colour Immunohistochemistry Kit	Akoya Biosciences	NEL811001KT
Software and algorithms		
Inform Advanced Image Analysis Software	PerkinElmer	
HALO	Indica Labs	
Other		
VectaShield HardSet Mounting Medium	Vector Labs	H-1400-10

EXPERIMENTAL MODEL AND STUDY PARTICIPANT DETAILS STUDY PARTICIPANTS

Stage III CRC primary tumor samples were retrospectively collected from patients including 218 females and 193 males with an average age of 61 (Table S1). Patients were recruited at Austin Health between 2008 and 2013 or provided by Victorian Cancer Biobank, for whom clinical, treatment and follow-up data were collected. TIL counts were derived from hematoxylin and eosin (H&E) stained whole tumor sections as previously described[19] and categorized as follows; TIL high tumors are described as >10 lymphocytes per 5 high powered fields (HPFs) and a low TIL count is defined as <10 lymphocytes per 5 HPFs. Only lymphocytes infiltrating the tumor epithelium were counted to generate the TIL score; stromal lymphocytes and lymphoid aggregates are not included or used to generate the TIL score. The 5 representative HPF were chosen at random, in accordance with the above criteria by an independent pathologist who is blinded to the sample and patient identification.

Tissue microarrays from 63 stage III CRC tumor samples were used for multiplex immunohistochemistry staining (31 female, 32 male, average age 68). For all other multiplex immunohistochemistry experiments involving human samples, FFPE whole tumor sections were used from both male and female patients. 20 whole tissue sections with high TIL counts were selected, of which ten were dMMR/microsatellite instability-high (MSI-H) and ten were mismatch repair proficient pMMR/microsatellite instability-low (MSI-L). Analysis of DNA mismatch repair status was performed using the Bethesda consensus panel of microsatellite markers as previously described.[19]

All human samples were collected and used in accordance with the procedures approved by the Austin Health Human Ethics Committee (Heidelberg, Australia protocol HREC/15/Austin/359 and 75462).

METHOD DETAILS

Multiplex immunohistochemistry (IHC)

Formalin-fixed paraffin-embedded (FFPE) whole tissue sections and TMAs of 0.4 μm thickness were stained using the Opal 7-Colour Immunohistochemistry Kit (Akoya Biosciences), according to the manufacturer's protocol, manually or using the Leica Bond RX Autostainer. Slides were stained with a combination of antibodies including CD3, CD8, Pan Cytokeratin, PD-1, TCF-1, TCRδ, CXCR5 and DAPI.

In summary, sections were baked, dewaxed and rehydrated. Antigen retrieval was performed at the corresponding pH, then slides were incubated with hydrogen peroxide (3%) and blocked with blocking buffer. The first cycle of primary antibody staining was performed, followed by HRP anti-mouse and rabbit-conjugated secondary antibody incubation and Opal signal development. The process was repeated with the

next sequential antibodies until complete, then nuclei were stained with DAPI. Upon completion, slides were set with VectaShield HardSet Mounting Medium (Vector Labs).

Imaging and analysis

Slides were imaged using the Vectra Imaging System (PerkinElmer). Whole slide scans of 10x magnification were acquired. Regions of interest were stamped using PhenoChart (PerkinElmer) to facilitate scanning of multispectral images (MSIs) of 20x magnification. For the whole tissue sections, MSIs were obtained for the tumor core, invasive front, lymphoid aggregates, tumor stroma and normal-adjacent tissue. For the TMAs, MSIs were acquired for every core. Image files were processed on the Inform Analysis software (PerkinElmer), then transferred to HALO (Indica Labs) to perform cell phenotyping. Cell frequencies and densities were calculated using cell counts, obtained from Halo. Lymphoid aggregates were defined as clusters of $CD3^+$ cells that are in direct contact with one another as previously described.[46] The cut off was set at >100 $CD3^+$ cells. This definition includes large lymphonets, immune hubs and tertiary lymphoid structures[16–19,45,46]. Frequencies of the $CD3^+$ cell populations were calculated based on the number of total cells, whereas the frequencies of $CD3^+CD8^+TCR\delta^-$ and $CD3^+CD8^-TCR\delta^+$ cell populations were calculated based on the total number of $CD3^+$ cells. This was performed for every region of interest (5 per patient), then the average per patient was plotted.

QUANTIFICATION AND STATISTICAL ANALYSIS

For all statistical analyses, GraphPad Prism 9.0 (GraphPad Software, San Diego, CA) was used. One-way analysis of variance (ANOVA), T-test or log rank (Mantel-Cox) tests were performed to determine statistical significance. All data are plotted as the means ± SEM, unless otherwise specified. p values <0.05 were considered statistically significant.